Research Article

Brief inhalation of sevoflurane can reduce glial scar formation after hypoxic-ischemic brain injury in neonatal rats

https://doi.org/10.4103/1673-5374.300456

Date of submission: January 31, 2020

Date of decision: March 7, 2020

Date of acceptance: May 26, 2020

Date of web publication: November 27, 2020

Qiu-Shi Gao, Ya-Han Zhang, Hang Xue, Zi-Yi Wu, Chang Li, Ping Zhao*

Graphical Abstract *Sevoflurane alleviates astrogliosis and glial scar formation after hypoxic-ischemic brain injury through stabilizing hypoxia-inducible factor-1α expression*

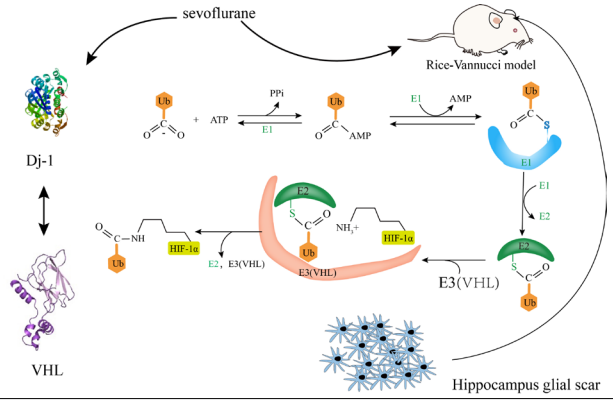

Abstract

Previous studies have demonstrated that sevoflurane postconditioning can provide neuroprotection after hypoxic-ischemic injury and improve learning and memory function in developing rodent brains. The classical Rice-Vannucci model was used to induce hypoxic-ischemic injury, and newborn (postnatal day 7) rats were treated with 2.4% sevoflurane for 30 minutes after hypoxic-ischemic injury. Our results showed that sevoflurane postconditioning significantly improved the learning and memory function of rats, decreased astrogliosis and glial scar formation, increased numbers of dendritic spines, and protected the histomorphology of the hippocampus. Mechanistically, sevoflurane postconditioning decreased expression of von Hippel-Lindau of hypoxia-inducible factor-1α and increased expression of DJ-1. Injection of 1.52 μg of the hypoxia-inducible factor-1α inhibitor YC-1 (Lificiguat) into the left lateral ventricle 30 minutes before hypoxic-ischemic injury reversed the neuroprotection induced by sevoflurane. This finding suggests that sevoflurane can effectively alleviate astrogliosis in the hippocampus and reduce learning and memory impairments caused by glial scar formation after hypoxic-ischemic injury. The underlying mechanism may be related to upregulated DJ-1 expression, reduced ubiquitination of hypoxia-inducible factor-1α, and stabilized hypoxia-inducible factor-1α expression. This study was approved by the Laboratory Animal Care Committee of China Medical University, China (approval No. 2016PS337K) on November 9, 2016.

Key Words: brain injury; brain; central nervous system; *in vivo*; injury; model; plasticity; rat; recovery; regeneration; repair

Chinese Library Classification No. R453; R741; R614.2+1

Introduction

Neonatal hypoxic-ischemic encephalopathy (HIE) is a common complication in the neonatal period caused by many factors, such as neonatal asphyxia, intrauterine distress, and hyaline membrane disease (Douglas-Escobar and Weiss, 2015; Barkhuizen et al., 2017). HIE is the leading cause of infant fatalities and the primary source of neurological sequelae (Edwards et al., 2010; Descloux et al., 2015). Ninety percent of HIE survivors have long-term neurological dysfunction, such as learning, cognitive, and motor dysfunctions, and epilepsy (Doi et al., 2012; Davies et al., 2019). Current treatment of HIE mainly focuses on symptomatic treatment, including mechanical ventilation, correction of hypotension, supplementation of glucose, and limiting of fluid intake, as appropriate. However, an effective treatment capable of reversing or reducing long-term brain damage is required (Stankowski and Gupta, 2011; Davidson et al., 2015).

As a pivotal part of learning and recognition, the hippocampus, including the dentate gyrus (DG), CA1, and CA3 regions, participates in transforming and integrating peripheral information into nerve centers (Morris et al., 2012; Jung et al., 2020). The hippocampus is hypersensitive to hypoxic-ischemic (HI) damage, which may provoke apoptosis of hippocampal neurons, stimulate excessive reactive gliosis, and lead to glial scar formation (Hopkins and Haaland, 2004; Wang et al., 2012). The proliferation of astrocytes is crucial for sealing the

Department of Anesthesiology, Shengjing Hospital of China Medical University, Shenyang, Liaoning Province, China

*Correspondence to: Ping Zhao, MD, PhD, zhaop@sj-hospital.org or zhaoping_sj@163.com.

https://orcid.org/0000-0001-6392-5391 (Ping Zhao)

Funding: *This study was supported by the National Nature Science Foundation of China, Nos. 81671311, 81870838; the Key Research and Development Program of Liaoning Province of China, No. 2018225004; and the Outstanding Scientific Fund of Shengjing Hospital of China, No. 201708 (all to PZ).*

How to cite this article: *Gao QS, Zhang YH, Xue H, Wu ZY, Li C, Zhao P (2021) Brief inhalation of sevoflurane can reduce glial scar formation after hypoxic-ischemic brain injury in neonatal rats. Neural Regen Res 16(6):1052-1061.*

site of infarction, remodeling the hippocampus structure, and temporally controlling local immune responses during the acute phase (Rolls et al., 2009). However, hypertrophy and glial scar formation contribute to aberrant neurogenesis, obstruct dendritic spine growth, and hamper synapse shape, further impairing learning and recognition functions (Yiu and He, 2006; Wanner et al., 2008; Burda and Sofroniew, 2014; Pekny et al., 2014; Shi et al., 2017). Glial fibrillary acidic protein (GFAP) and chondroitin sulfate proteoglycans, such as neurocan, are pathologic markers of astrogliosis and glial scarring whose expression can be upregulated by highly activated astrocytes (Pekny and Nilsson, 2005; Choudhury and Ding, 2016). Thus, inhibition of astrogliosis and glial scarring may be a therapeutic target for HIE and its long-term neurological sequelae.

The application of sevoflurane has been demonstrated to mitigate HI injury in rodents. Studies investigating the significance of sevoflurane postconditioning (SPC) to alleviate HI damage by upregulating hypoxia-inducible factor-1α (HIF-1α) in adult rodents and neonatal rats have identified several potential mechanisms (Wang et al., 2019b; Yang et al., 2019; Du et al., 2020; Liu and Gong, 2020). As a key physiological sensor of hypoxia, HIF-1α is a transcription factor with hundreds of downstream molecules involved in ischemic tolerance mechanisms, such as vascular endothelial growth factor and erythropoietin (Na et al., 2015). Hypoxic postconditioning has been verified to reduce astrocyte and microglial activation after HI in neonatal rat brain (Teo et al., 2015). Therefore, we hypothesized that HIF-1α may contribute to attenuating the formation of glial scars and astrogliosis.

HIF-1α can constitutively exist in neurons, whereby it quickly increases in expression and accumulates under hypoxic conditions. However, when oxygen returns to normal, HIF-1α expression cannot be sustained at a high enough level to continuously exert a neuroprotective effect because of oxygen-dependent degradation by prolyl-hydroxylase proteins and subsequent ubiquitylation by von Hippel-Lindau (VHL) proteins (Berra et al., 2003; Zhang et al., 2018). DJ-1 (encoded by Park7) is reportedly a neuroprotective protein, especially under oxidative conditions (Aleyasin et al., 2007, 2010). VHL protein physically interacts with DJ-1, as determined by an unbiased mass spectrometry screen and confirmed in a Parkinson's disease (PD) model. In addition, Parsanejad et al. (2014) showed that DJ-1 inhibits VHL-dependent ubiquitylation and stabilizes HIF-1α expression. Thus, we hypothesized that sevoflurane stabilizes HIF-1α protein in the hippocampus by upregulating DJ-1 to inhibit HIF-1α ubiquitylation, thereby improving long-term learning and memory function. To investigate the role of HIF-1α in the relationship between sevoflurane and astrogliosis, we used YC-1 (Lificiguat), a selective antagonist of HIF-1α, to completely inhibit HIF-1α expression at the post-transcriptional level. In this study, we investigated the role of HIF-1a in neuroprotection of SPC-treated HIE neonatal rats.

Materials and Methods

Animals

Animal research was performed at the synaptic stage of rat development, which commences on postnatal day 7 (P7), corresponding to the growth period of human infants from late pregnancy to 3 years after birth (Jevtovic-Todorovic et al., 2003). Seven-day-old Sprague-Dawley rats weighing 12–16 g were selected from 20 pregnant rats (purchased from the Laboratory of Shengjing Hospital, China Medical University, China; male/female ratio, 1:1). All rats were able to access water and food freely, and maintained at standard humidity and temperature in the lab, with 12-hour light/dark (8 a.m./8 p.m.) cycles. All animal experiments were performed according to the National Institutes of Health (Bethesda, MD, USA) Guidelines for the Care and Use of Laboratory Animals. The Laboratory Animal Care Committee of China Medical University formally approved the described experiments (Shenyang, China; approval No. 2016PS337K) on November 9, 2016.

From 25 pregnant rats, 249 P7 rats were chosen and randomly divided into groups based on a random number table (Wang et al., 2019a). Our final analysis included a total of 201 newborn rats; the mortality rate after HI treatment was 19%. These 201 newborn rats were randomly divided into four groups: sham (n = 54), HI (n = 54), HI + sevoflurane (HIS) (n = 54), and HIS + YC-1 (n = 39) groups. In each group, 24 rats were used for western blot assay, 5 were used for immunohistochemistry and Golgi staining, and 10 were used for behavioral testing. The remaining 45 rats in sham, HI, and HIS groups were used for reverse transcription polymerase chain reaction (RT-PCR).

Experimental design and exposure to anesthetic

The employed HIE model was previously described (Zhao et al., 2007; Grandvuillemin et al., 2017). On the basis of the distance between the anus and reproductive organs, sex identification of postnatal rats was completed. To establish the HIE model, the head of each P7 rat was put into a transparent plastic pipe, which was sealed with cotton before sevoflurane was released (Wang et al., 2019a; Xue et al., 2019). The left common carotid artery of each rat was permanently ligated, and between the two ligations, the artery was cut; each surgery was finished within 5 minutes. Subsequently, the rats awoke unaffected by anesthesia and were put back into their mothers' cage for 2 hours.

For administration of SPC, rats were put into a transparent chamber (Lingzhi Company, Hangzhou, China) connected to a sevoflurane vaporizer; one duct assisted in ventilation, while the other conveyed the gas sample out of the chamber to the monitor. The chamber was ventilated with 30% O_2 and 70% N_2 for 2 hours for the sham group, while 8% O_2 and 92% N_2 was administered for 2 hours to the HI group. SPC was set promptly after HI: 2.4% sevoflurane (1 minimum alveolar concentration) was inhaled by rats in the chamber with an atmosphere of 30% O_2 and 70% N_2 and air flow rate of 2 L/min for 30 minutes. The heating pool stabilized the temperature inside the chamber at 37°C.

Drug administration

Exactly 30 minutes before HI, 1.52 μg of HIF-1α inhibitor (YC-1; Sigma-Aldrich, St. Louis, MO, USA) was injected into the left lateral ventricle (Paxinos and Franklin, 2013) using a 5-μL Hamilton syringe (Yingweida Technology, Beijing, China). As previously described, YC-1 was dissolved in artificial cerebral spinal fluid at a concentration of 0.304 μg/μL (Shen et al., 2012; Na et al., 2015).

Western blot analysis

P7 rats were anesthetized by 2% sevoflurane, and hippocampal tissues were extracted from pups at 12, 24, and 48 hours, and 28 days after surgery. After extraction, tissues were immediately placed on ice. Total supernatant proteins were isolated by adding radio-immunoprecipitation assay agent (Beyotime, Haimen, China). Protein concentrations were determined with a One BCA Kit (Beyotime). Next, specimens were separated on 12.5% sodium dodecyl sulfate-polyacrylamide gels and transferred to nitrocellulose membranes. After blocking with 5% bovine serum albumin (Sigma-Aldrich) at 4°C, the membrane was incubated with the appropriate primary antibodies, including anti-glyceraldehyde

3-phosphate dehydrogenase (GAPDH; 1:2000; Cat# 5174S; Cell Signaling Technology, Danvers, MA, USA), anti-DJ-1 (1:1000; Cat# ab18257; Abcam, Cambridge, UK), anti-VHL (1:5000; polyclonal; Cat# ab77262; Abcam), anti-HIF-1α (1:900; polyclonal; Cat# ab2185; Abcam), anti-neurocan (1:200; monoclonal; Cat# sc-33663; Santa Cruz Biotechnology, Dallas, TX, USA), anti-postsynaptic density protein 95 (PSD95; 1:1000; monoclonal; Cat. No 3409S; Cell Signaling Technology), anti-growth associated protein 43 (GAP43; 1:2000; polyclonal; Cat# 16971-1-AP; Proteintech Biotechnology, Chicago, IL, USA), and anti-GFAP (1:5000, polyclonal, Cat# ab53554; Abcam). Afterwards, blots were incubated with anti-rabbit IgG (1:5000; Cat# ZB-2301; Zhongshanjinqiao, Beijing, China) or anti-mouse IgG (1:5000; Cat# ZB-2301; Zhongshanjinqiao) for 2 hours at room temperature. Protein blots were visualized with enhanced chemiluminescence detection reagents (Super Signal West Pico; Pierce, Rockford, IL, USA). Protein bands were quantified with ImageJ software (National Institutes of Health). For analysis of western blots, data were normalized to GAPDH.

Immunohistochemistry

Twenty-eight days after surgery, rats were administered anesthetic using the method described above, perfused with 4% formalin, and their brains were removed for immunofluorescence staining. Brains were immersed into 4% paraformaldehyde at 4°C for 48 hours, subsequently dehydrated in a graded ethanol series, and finally embedded in paraffin. Next, paraffin-embedded tissues were cut into 2.5-μm-thick sections with a vibratome, and the resulting sections were stored at room temperature. Each brain was sectioned continuously, and three discontinuous brain sections were selected for NeuN (neuron marker), GFAP (astrocyte marker), and neurocan (glial scar marker) staining. For double labeling, tissue sections were incubated with two mixed primary antibodies, including goat anti-GFAP (1:250; polyclonal; Cat# ab53554; Abcam), rabbit anti-NeuN (1:100; Cat# 12943; Cell Signaling Technology), and/or mouse anti-neurocan (1:200; monoclonal; Cat# sc-33663; Santa Cruz Biotechnology) at 4°C overnight in a humidified chamber. Subsequently, sections were washed with 0.1 M phosphate-buffered saline and incubated for 2 hours at room temperature with the appropriate secondary antibodies, including anti-rabbit IgG conjugated to Alexa Fluor-594 (1:200; Life Technologies, Grand Island, NY, USA), anti-mouse IgG conjugated to Alexa Fluor-594 (1:200; Life Technologies), and anti-goat IgG conjugated to fluorescein isothiocyanate (1:200; Life Technologies). Counterstaining of cell nuclei was implemented with 4′,6-diamidino-2-phenylindole (Beyotime) for 5 minutes. An Olympus BX51 microscope (Olympus Corporation, Tokyo, Japan) was used for the observation of stained sections. Three fields of view of the left hippocampus were randomly selected from each slice for photography. ImageJ software was utilized to estimate quantitative colocalization and, therefore, calculate Manders' overlap coefficient.

Real-time PCR

Total RNA was extracted from the hippocampal tissues of pups at 12, 24, and 48 hours after surgery using TRIzol reagent (Invitrogen, Carlsbad, CA, USA). Complementary DNA was synthesized using an advanced Superscript II RT-PCR kit (Invitrogen). Fluorescent SYBR Green I dye (SYBR Green PCR Master Mix, Applied Biosystems, Foster City, CA, USA) and 1 μL of reverse transcribed complementary DNA were used to detect DNA synthesis by real-time PCR with HIF-1α-specific primers. In the rotor gene real-time DNA amplification system (Corbett Research, Sydney, Australia), PCR was performed with the following cycles: denaturation at 95°C for 15 minutes; 40 cycles of 95°C (20 seconds), annealing at 58°C for 25 seconds, and pull-down at 72°C for 35 seconds. Monitoring of the fluorescent product was carried out for an extended time at 72°C. Rotor gene analysis software (Corbett Research) was used to standardize the housekeeping gene GAPDH and quantify relative gene expression. All primer sequences are shown in **Table 1**.

Nissl staining

Rat brains were prepared into slices 28 days after surgery as described above for immunohistochemistry. Each brain was sectioned consecutively, and three similar sections of the brain were selected for Nissl staining. Utilizing a Nikon C1 digital microscope camera (Nikon Corporation, Tokyo, Japan), typical microphotographs of hippocampal CA1, CA3 and DG areas were captured. Numbers of cells was counted in each of the three sections was performed in a blinded manner using ImageJ software.

Behavioral tests

Rats were weaned at 3 weeks, divided into three to five groups, and kept in cages according to group assignment. Behavioral tests were conducted on P28–P33 (i.e. 21–26 days after surgery) rats, as previously described (Wang et al., 2019a) but with slight modification. To exclude the influence of the estrous cycle on rodent behavior, only male rats were tested.

Morris water maze

Morris water maze testing was used to evaluated the spatial learning and memory abilities of P28–P33 rats (Wang et al., 2019a). Testing consisted of two phases including the training section and spatial searching test. For 5 consecutive days, four training sections were implemented daily commencing at 8:00 am. For platform-detection testing, 10 rats from each group were individually placed into the water at various locations, stochastically, facing the wall of the pool. If a rat successfully detected the platform within 90 seconds, it was forced to stay on the platform for 20 seconds and the time taken to detect the platform was recorded as the escape latency. Each round of testing was 90 seconds, and the escape latency was measured as the time from the rat being placed in the water to successful boarding of the platform. If the rat failed to find the platform within 90 seconds, the recording was stopped and learning and memory guidance was performed (the experimenter used a long rod to guide the rat to the platform and allowed them stay on the platform for 20 seconds to learn). During the test, the escape latency of rats who failed to enter the stage was recorded as 90 seconds. In the spatial probe test implemented on the sixth day of testing, the platform was removed and the rat was placed in the opposite quadrant and permitted to swim for 90 seconds. The speed of swimming, escape latency, and number of times that they crossed the place where the platform was previously located were recorded by the video tracking system (Shanghai Mobile Datum Ltd., Shanghai, China).

Table 1 | **Primers for real-time reverse transcription polymerase chain reaction**

Gene	Primer sequence (5′–3′)	Accession No.
HIF-1α	Forward: CCG GGG GAG GAC GAT GAA CA	NM_024359.1
	Reverse: TGA ATG TGG CCC GTG CAG TGA AG	
GAPDH	Forward: AAT GCA TCC TGC ACC ACC AA	NM_130405
	Reverse: GAT GGC ATG GAC TGT GGT CA	

GAPDH: Glyceraldehyde 3-phosphate dehydrogenase; HIF-1α: hypoxia-inducible factor-1α.

Suspension test

The suspension test was performed on P28–P32 rats to evaluate their motor function, starting at 3 p.m. every day. A horizontal plastic rope with a 0.5-cm diameter was placed at a 45-cm distance from the ground, and rats were guided to hold the plastic rope with both upper limbs, at which point the time until the rat fell was measured as the suspension latency. The test ended if: (i) the rat tumbled; (ii) the suspension latency was more than 60 seconds; or (iii) the rope was caught by posterior limbs.

Open field test

Open field testing was conducted on P28 rats using outdoor equipment composed of a Plexiglas box (100 cm × 100 cm; Borj Sanat, Tehran, Iran) surrounded by a 45-cm high wall, with a floor split into 16 squares. The central area was the 50 cm × 50 cm area in the center of the arena. Each rat was individually placed in the center of the arena and permitted to explore without limitations for 10 minutes. A video tracking system (Borj Sanat) was utilized to record and analyze the total itinerary (as an indicator of exercise activity) and time spent in the central area (as an indicator of anxiety behavior) (Zhai et al., 2019).

Golgi staining

After the completion of behavioral testing (i.e. 26 days after surgery), five rats were randomly selected from each group. Golgi staining was performed on 150-μm-thick frozen brain sections using an FD Rapid Golgi Stain Kit (FD NeuroTechnologies, Columbia, MD, USA) according to the manufacturer's protocol. ImageJ software was utilized to analyze the spine density (spine number per 10 μm) of each neuron. Spines were counted on two or three secondary dendrite segments.

Statistical analysis

SPSS 17.0 for Windows (SPSS Inc., Chicago, IL, USA) was used to analyze the data, which are shown as mean ± standard error of mean (SEM). The Shapiro-Wilk test was used to test the assumption of normality among all continuous variables. In addition, one-way analysis of variance followed by Tukey's *post hoc* multiple comparison tests was approached in a string of experiments. If the data failed to meet the normality assumption, the Kruskal-Wallis *H* test or Mann-Whitney *U* test was completed separately. Escape latency was analyzed on the basis of two-way analysis of variance for iterative measurements. *P* values < 0.05 were regarded as statistically significant.

Results

SPC improves hippocampal neuronal cell loss

The hippocampus, including the three examined regions, is associated with learning and memory (Jung et al., 2020). After behavioral testing, Nissl staining was performed to examine hippocampal architecture. In the HI group, viable neuronal density was reduced compared with the sham group. However, numbers of neurons were increased in animals exposed to SPC; this effect was reversed by YC-1, which reduced neuronal density (**Figure 1A**). This phenomenon was observed in CA1, CA3 and DG regions of the hippocampus ($P < 0.05$; **Figure 1B–D**).

SPC improves reduces dendritic spine density in the hippocampal CA1 area

Golgi staining was used to detect CA1 pyramidal neuronal dendritic spine density (**Figure 2A**). Because the sizes of spines greatly varied (e.g., branched dendrites, thin or mushroomed), we only determined that the density of dendritic spines was significantly increased in the HIS group compared with the HI group ($P < 0.05$), while the density of dendritic spines was reduced in the HIS + YC-1 group compared with the HIS group ($P < 0.01$; **Figure 2B**).

SPC ameliorates PSD95 and GAP43 expression in the hippocampus

We evaluated expression of synapse-associated proteins GAP43 and PSD95 to determine whether they were inhibited by glial scars. HI significantly reduced PSD95 ($P < 0.01$) and GAP43 ($P < 0.05$) protein expression compared with the sham group (**Figure 2C–E**). Compared with the HIS group, expression levels of PSD95 and GAP43 were notably decreased after YC-1 injection.

Formation of astrogliosis and glial scars obviously damages hippocampal architecture after HI

Next, we tried to verify whether sevoflurane improved learning and memory function by protecting the hippocampal architecture and attenuating astrogliosis. Neonatal HIE induced neuronal apoptosis in the hippocampus, as well as reactive astrogliosis in the infarct region that subsequently develops into a glial scar (Rolls et al., 2009). In the HI group, the CA1 and CA3 pyramidal layers, and DG region showed obvious decreases in neurons ($P < 0.01$, $P < 0.001$; **Figures 3E** and **4C**), as well as increased numbers of astrocytes with distinct morphological changes ($P < 0.001$; **Figures 3C** and **4B**). We evaluated expression of GFAP and NeuN in the three areas of the left hippocampus using immunohistochemistry and western blotting analysis. Our results showed that compared with the sham group, astrocytes were activated in the HI group, inserted into the CA1 (**Figure 4A**) and CA3 (**Figure 3A**) pyramidal layer, and surrounded neurons in the DG (**Figure 3B**). Excessive astrogliosis resulted in further extension of glial processes towards normal neuronal structures, forming an aberrant wall-like astrocyte net (**Figures 3A**, **B** and **4A**). Moreover, GFAP immunoreactivity (**Figures 3C**, **D** and **4B**, **E**) and protein levels were obviously increased ($P < 0.01$; **Figure 4E**), while NeuN immunoreactivity was decreased ($P < 0.01$ or $P < 0.001$; **Figures 3E**, **F** and **4C**).

To further verify glial scar formation, we evaluated neurocan protein expression levels and immunoreactivity in the hippocampus (**Figures 5A**, **B** and **6A**). Results of double-labeling immunofluorescence revealed notable differences in the fluorescence intensity of neurocan$^+$/GFAP$^+$ immunostaining between HI and sham groups ($P < 0.001$, $P < 0.05$, $P < 0.01$; **Figures 5G**, **H** and **6D**), consistent with western blot results ($P < 0.01$; **Figure 6F**).

SPC attenuates astrogliosis and glial scar formation in the hippocampus

Next, our study investigated whether SPC attenuated glial scar formation. Compared with the HI group, immunoreactivity of GFAP (**Figures 5C**, **D** and **6C**) and neurocan (**Figures 5E**, **F** and **6B**) in the HIS group was markedly downregulated in the hippocampus ($P < 0.01$ or $P < 0.001$). In contrast, GFAP and neurocan expression in the HIS + YC-1 group was notably increased compared with the HIS group, and was not different from HIS + YC-1 and HI groups ($P > 0.05$; **Figure 6E** and **F**). In addition, NeuN immunopositivity was upregulated and structures appeared more orderly in the HIS group compared with the HI group, which was reversed by YC-1 (**Figures 3E**, **F** and **4C**).

SPC upregulates HIF-1α expression in the hippocampus

In a previous study, we found that sevoflurane post-

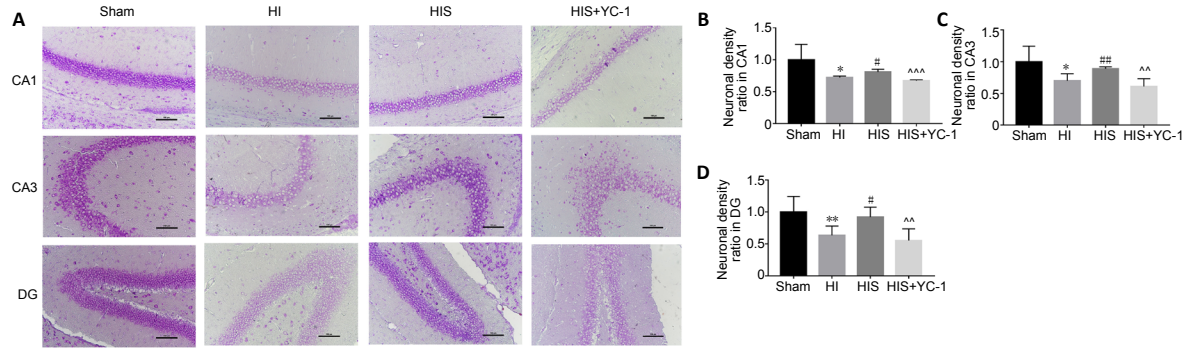

Figure 1 | **Effect of sevoflurane on hippocampal neuronal cells in newborn rats with hypoxic-ischemic injury.**
(A) Nissl staining of hippocampal neuronal cells (original magnification 200×, scale bars: 100 μm). The neuronal density in HI and HIS + YC-1 groups was reduced compared with sham and HIS groups. Viable cells showed apparent significant elliptical nuclei (stained light blue) and visible nucleoli, with profuse Nissl substance and cytoplasm (stained light purple); whereas, apoptotic or necrotic cells showed irregular morphology, with amorphous nuclei. (B–D) Neuronal density ratio in hippocampal CA1 (B), CA3 (C), and DG (D) areas. Data are expressed as mean ± SEM (n = 5 in each group). *P < 0.05, **P < 0.01, *vs*. sham group; #P < 0.05, ##P < 0.01, *vs*. HI group; ^^P < 0.01, ^^^P < 0.001, *vs*. HIS group (one-way analysis of variance followed by Tukey's *post hoc* test). DG: Dentate gyrus; HI: hypoxic-ischemic; HIS: hypoxic-ischemic + sevoflurane; YC-1: Lificiguat, a hypoxia-inducible factor-1α inhibitor.

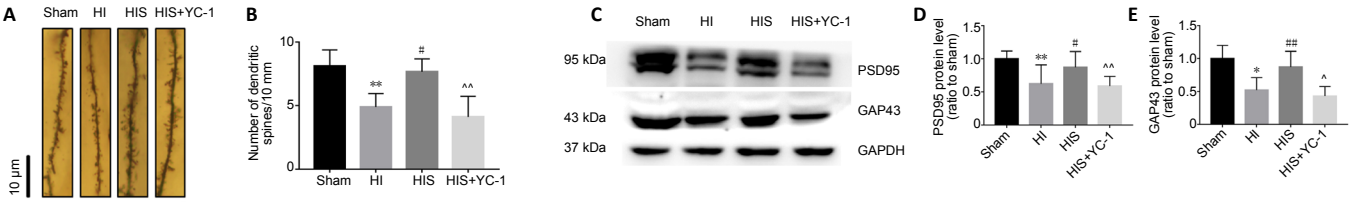

Figure 2 | **Effect of sevoflurane on dendritic spines in the hippocampal CA1 area of newborn rats with hypoxic-ischemic injury.**
(A) Golgi staining in the hippocampal CA1 area (original magnification 1000×, scale bars: 10 μm). The density of dendritic spines in the HIS group was higher than that observed in HI and HIS + YC-1 groups. (B) Number of dendritic spines. (C) Bands of PSD95 and GAP43 detected by western blot assay. (D, E) Relative expression of PSD95 (D) and GAP43 (E). Data are expressed as mean ± SEM (n = 6 in each group). *P < 0.05, **P < 0.01, *vs*. sham group; #P < 0.05, ##P < 0.01, *vs*. HI group; ^P < 0.05, ^^P < 0.01 *vs*. HIS group (one-way analysis of variance followed by Tukey's *post hoc* test). GAP43: Growth associated protein 43; GAPDH: glyceraldehyde 3-phosphate dehydrogenase; HIS: hypoxic-ischemic + sevoflurane; HI: hypoxic-ischemic; PSD95: postsynaptic density protein 95; YC-1: Lificiguat, a hypoxia-inducible factor-1α inhibitor.

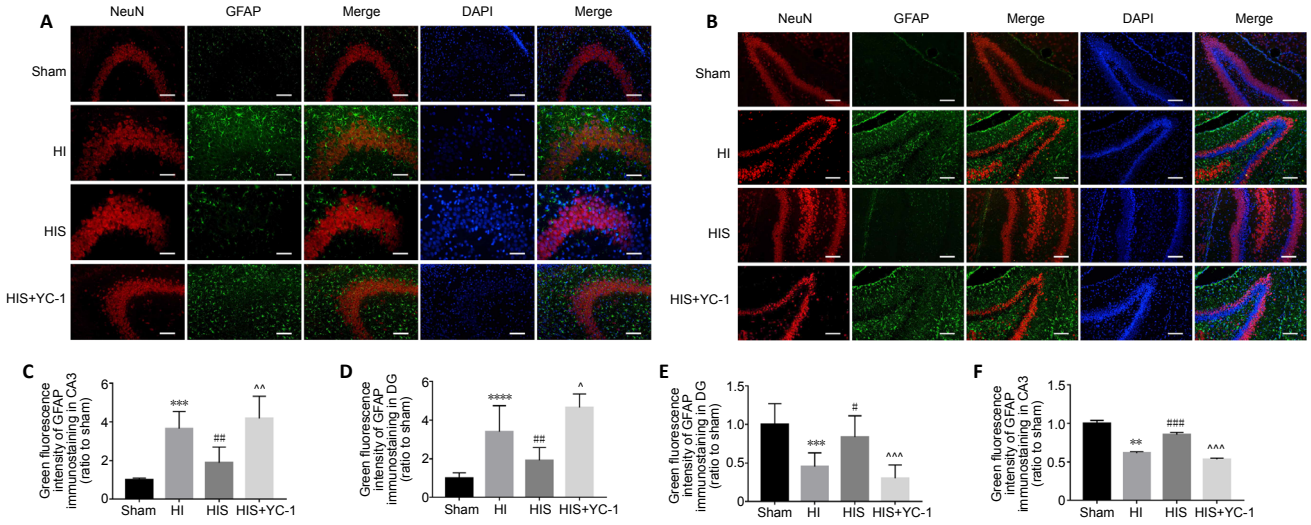

Figure 3 | **Effect of sevoflurane on astrocytes and neurons in the hippocampal CA3 and DG areas of newborn rats with hypoxic-ischemic injury.**
(A, B) Morphological changes in astrocytes and neurons in hippocampal CA3 (A) and DG (B) areas 28 days after injury. Astrocytes in the HIS group were more regular than those observed in HI and HIS + YC-1 groups, while neurons were denser. GFAP: Green (fluorescein isothiocyanate); neuron: $NeuN^+$ cells, red (Alexa Fluor-594); DAPI: blue. Scale bars: 50 μm. (C, D) Immunopositivity of GFAP in hippocampal CA3 (C) and DG (D) areas. (E, F) Immunopositivity of NeuN in hippocampal DG (E) and CA3 (F) areas. Data are expressed as mean ± SEM (n = 5 in each group). **P < 0.01, ***P < 0.001, ****P < 0.0001, *vs*. sham group; #P < 0.05, ##P < 0.01, ###P < 0.001, *vs*. HI group; ^P < 0.05, ^^P < 0.01, ^^^P < 0.001, *vs*. HIS group (one-way analysis of variance followed by Tukey's *post hoc* test). DAPI: 4′,6-Diamidino-2-phenylindole; DG: dentate gyrus; GFAP: glyceraldehyde 3-phosphate dehydrogenase; HI: hypoxic-ischemic; HIS: hypoxic-ischemic + sevoflurane; YC-1: Lificiguat, a hypoxia-inducible factor-1α inhibitor.

conditioning attenuated astrogliosis and glial scar formation in the hippocampus, and improved learning and memory impairment after HI. HIF-1α was confirmed as a key factor in this neuroprotective mechanism (Yang et al., 2019).

To further investigate the specific regulation induced by sevoflurane, we examined HIF-1α protein expression in the hippocampus 12, 24, and 48 hours after SPC. Our results revealed dynamic changes in HIF-1α expression: 12 hours after treatment, increased HIF-1α expression was observed in HI and HIS groups compared with the sham group (P < 0.0001),

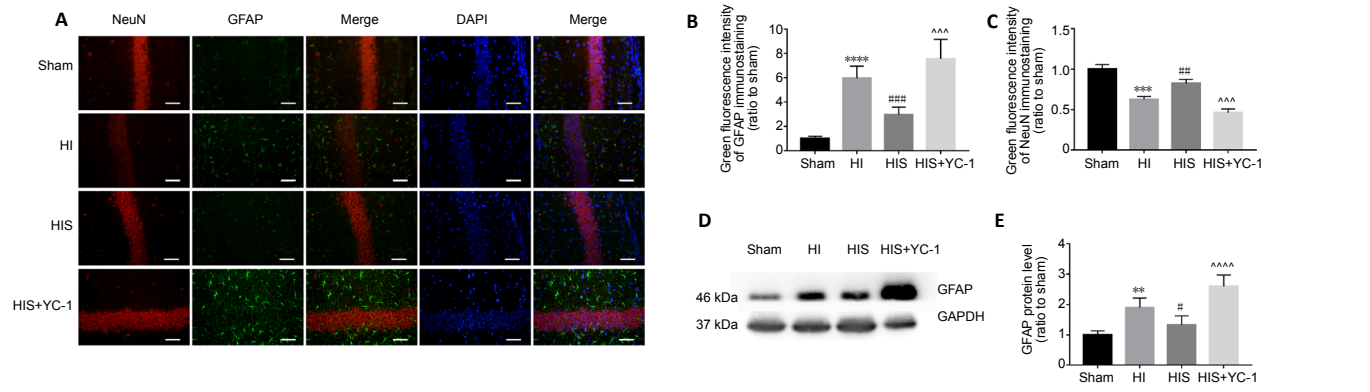

Figure 4 | **Effect of sevoflurane on astrocytes and neurons in the hippocampal CA1 of newborn rats with hypoxic-ischemic injury.**
(A) Morphological changes in astrocytes and neurons in the hippocampal CA1 area 28 days after injury. Astrocytes in the HIS group were more regular than those observed in HI and HIS + YC-1 groups, while neurons were denser. GFAP: green (fluorescein isothiocyanate); neuron: $NeuN^+$ cells, red (Alexa Fluor-594); DAPI: blue. Scale bars: 50 μm. (B, C) Immunopositivity of GFAP (B) and NeuN (C) in the hippocampal CA1 area. (D) Bands of GFAP detected by western blot assay. (E) Relative expression of GFAP. Data are expressed as mean ± SEM (n = 5 in each group). $^{**}P < 0.01$, $^{***}P < 0.001$, $^{****}P < 0.0001$, *vs*. sham group; #P < 0.05, ##P < 0.01, ###P < 0.001, *vs*. HI group; ^^^P < 0.001, ^^^^P < 0.0001, *vs*. HIS group (one-way analysis of variance followed by Tukey's *post hoc* test). DAPI: 4′,6-Diamidino-2-phenylindole; GFAP: glyceraldehyde 3-phosphate dehydrogenase; HI: hypoxic-ischemic; HIS: hypoxic-ischemic + sevoflurane; YC-1: Lificiguat, a hypoxia-inducible factor-1α inhibitor.

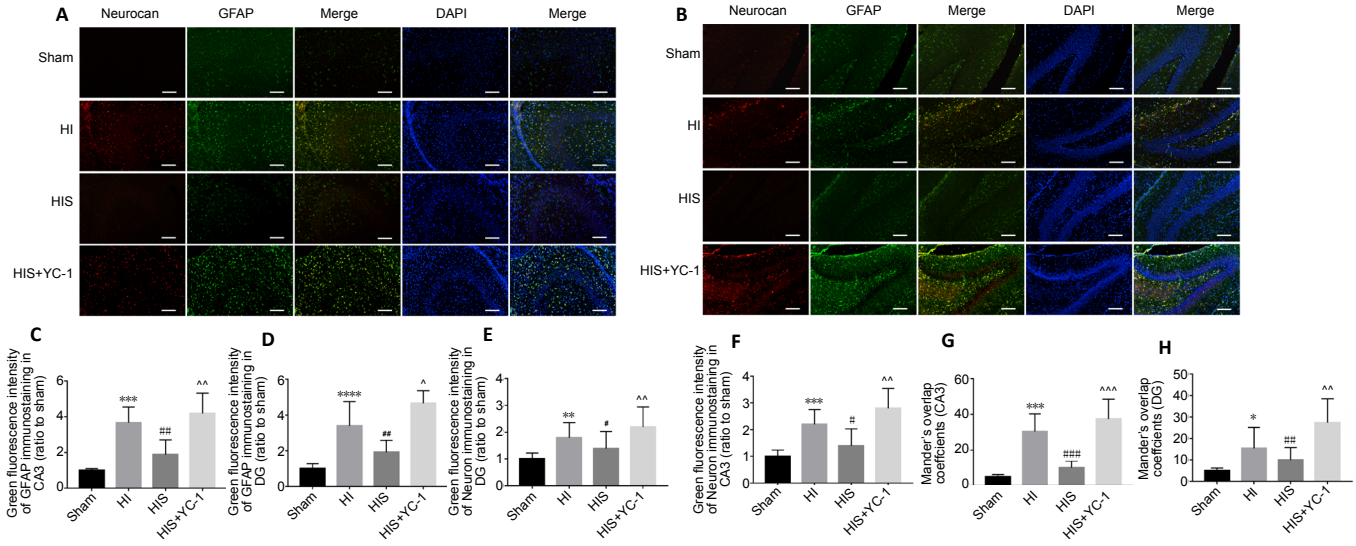

Figure 5 | **Effect of sevoflurane on glial scar formation in the hippocampal CA3 and DG areas of newborn rats with hypoxic-ischemic injury.**
(A, B) Neurocan and GFAP in hippocampal CA3 (A) and DG (B) areas at 28 days after injury. The glial scar in CA3 and DG areas in HI and HIS+YC-1 groups were more obvious than those observed in the HIS group. Neurocan: red (Alexa Fluor-594); GFAP: green (fluorescein isothiocyanate); DAPI: blue. Scale bars: 50 μm. (C, D) Immunopositivity of GFAP in hippocampal CA3 (C) and DG (D) areas. (E, F) Immunopositivity of neurocan in hippocampal DG (E) and CA3 (F) areas. (G, H) Manders' overlap coefficient demonstrated co-localization between neurocan and GFAP in hippocampal CA3 (G) and DG (H) areas. Data are expressed as mean ± SEM (n = 5 in each group). *P < 0.05, **P < 0.01, ***P < 0.001 *vs*. sham group; #P < 0.05, ##P < 0.01, ###P < 0.001, *vs*. HI group; ^P < 0.05, ^^P < 0.01, ^^^P < 0.001, *vs*. HIS group (one-way analysis of variance followed by Tukey's *post hoc* test). DAPI: 4′,6-Diamidino-2-phenylindole; DG: dentate gyrus; GFAP: glyceraldehyde 3-phosphate dehydrogenase; HI: hypoxic-ischemic; HIS: hypoxic-ischemic + sevoflurane; YC-1: Lificiguat, a hypoxia-inducible factor-1α inhibitor.

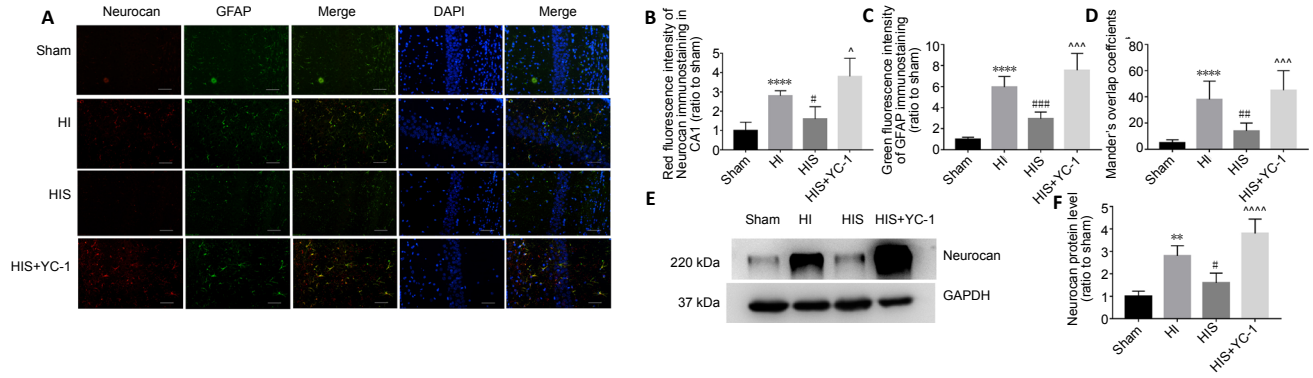

Figure 6 | **Effect of sevoflurane on glial scar formation in the hippocampal CA1 area of newborn rats with hypoxic-ischemic injury.**
(A) Neurocan and GFAP in the hippocampal CA1 area at 28 days after injury. Glial scars in the CA1 area in HI and HIS+YC-1 groups were more obvious than those observed in the HIS group. Neurocan: red (Alexa Fluor-594); GFAP: green (fluorescein isothiocyanate); DAPI: blue. Scale bars: 50 μm. (B, C) Immunopositivity of neurocan (B) and GFAP (C) in the hippocampal CA1 area. (D) Manders' overlap coefficient demonstrated co-localization between neurocan and GFAP. (E) Bands of neurocan detected by western blot assay. (F) Relative expression of neurocan. Data are expressed as mean ± SEM (n = 5 in each group). **P < 0.01, ****P < 0.0001, *vs*. sham group; #P < 0.05, ##P < 0.01, ###P < 0.001, *vs*. HI group; ^P < 0.05, ^^^P < 0.001, ^^^^P < 0.0001, *vs*. HIS group (one-way analysis of variance followed by Tukey's *post hoc* test). DAPI: 4′,6-Diamidino-2-phenylindole; GFAP: glyceraldehyde 3-phosphate dehydrogenase; HI: hypoxic-ischemic; HIS: hypoxic-ischemic + sevoflurane; YC-1: Lificiguat, a hypoxia-inducible factor-1α inhibitor.

but there were virtually no differences between HI and HIS groups (**Figure 7A** and **B**). Twenty-four hours after SPC, HIF-1α expression was decreased in the HI group compared with the HIS group ($P < 0.001$), but still increased compared with the sham group ($P < 0.001$; **Figure 7C**). Forty-eight hours after SPC, HIF-1α expression in the HI group returned to a very low level and was not different from the sham group; however, HIF-1α expression was still sustained at a very high level in the HIS group ($P < 0.01$; **Figure 7D**).

Next, we examined expression of HIF-1α mRNA (relative to GAPDH) in the hippocampus 12, 24, and 48 hours after SPC by real-time PCR analysis. The results revealed that HIF-1α mRNA expression peaked 24 hours after HI ($P < 0.001$; **Figure 7E**), and there were no obvious differences between HI and HIS groups at the three time points examined. Thus, the dynamic regulation of HIF-1α induced by sevoflurane probably involved post-translational regulation, which is in line with our hypothesis.

To further investigate our hypothesis that SPC reduces astrogliosis after HI injury in neonatal rats by upregulating DJ-1 to inhibit HIF-1α ubiquitylation, we examined expression of VHL and DJ-1 proteins (**Figure 8A**). VHL protein physically interacts with DJ-1 (Parsanejad et al., 2014), as analyzed in an unbiased mass spectrometry screen and confirmed in a PD model. Our findings indicated that DJ-1 could inhibit VHL-dependent ubiquitylation and stabilize HIF-1α expression. Moreover, our results showed that VHL expression decreased when DJ-1 expression was increased in the HIS group compared with the HI group ($P < 0.05$; **Figure 8B** and **C**).

HIF-1α inhibitor YC-1 attenuates improvement of learning and memory induced by sevoflurane

Neonatal HIE leads to many negative long-term effects; one of the most severe dysfunctions is the impairment of learning and memory. Abundant evidence has demonstrated that SPC can protect against HI damage and improve learning and memory function (Wang et al., 2019a; Xue et al., 2019; Yang et al., 2019). We injected YC-1, an inhibitor of HIF-1α, to verify whether the protective mechanism of sevoflurane is related to HIF-1α. The Morris water maze was used to evaluate learning and recognition on days 29–34 after surgery (**Figure 9A**). There were manifest differences in escape latency between HI and HIS groups ($P < 0.0001$). YC-1 treatment notably increased escape latency after sevoflurane exposure ($P < 0.01$; **Figure 9B**). In the spatial probe test, the HIS group performed better than HI ($P < 0.01$) and HIS + YC-1 ($P < 0.05$; **Figure 9C**) groups. However, the YC-1 injection group did not show marked improvement compared with the HI group. Apart from this, no motor impairment was observed according to swimming speed or suspension test results ($P > 0.05$; **Figure 9D** and **E**). Open field test results revealed no differences in time spent in the center or total distance traveled between groups ($P > 0.05$; **Figure 9F–H**), indicating there was no locomotor activity or anxiety behavior divergence among the four groups.

Discussion

The classical Rice–Vannucci model was used in this study to evaluate the effects of SPC on HIE in P7 rats (Jevtovic-Todorovic et al., 2003; Grandvuillemin et al., 2017). Our results showed that: (1) SPC improved long-term learning and memory in neonatal HIE by attenuating excessive hippocampal astrogliosis and glial scarring; (2) sevoflurane may induce the observed neuroprotection by stabilizing HIF-1α expression through inhibition of its ubiquitylation; and (3) inhibition of HIF-1α ubiquitylation by sevoflurane may be induced via upregulation of DJ-1, which has been demonstrated to be neuroprotective in PD (Parsanejad et al., 2014) and is regulated by SPC. Glial scars affect neuronal alignment and synapse generation in the developing brain. Herein, we found that sevoflurane upregulates the brain protective protein DJ-1, reduces the level of HIF-1α ubiquitination, improves glial scarring, and affects long-term learning and memory functions to exert brain protection.

Most live-born babies surviving HIE suffer severe neurological dysfunction, such as cerebral palsy, epilepsy, and especially long-term learning and memory impairment (Edwards et al., 2010; Descloux et al., 2015). However, current treatment of HIE mainly focuses on symptomatic treatment (Yuan, 2009). Only a few treatments, such as whole-body moderate hypothermia, can provide neuroprotection and improve long-term outcomes. Application of the inhaled anesthetic sevoflurane after neonatal HIE provides neuroprotection that can reverse the damage caused by HI, as verified in animal studies (Lai et al., 2016; Kim et al., 2017). The influence of anesthetics on the developmental nervous system has also been a hot topic of research for many years (Archer et al., 2017). The effects of inhaled anesthetics on the brain are concentration-dependent. Low-concentration and short-term treatments have protective effects on the injured brain, while high-concentration and long-term treatments can damage brain tissue. However, the mechanism underlying protection from brain damage has not yet to be clarified. Therefore, we explored the potential mechanisms of sevoflurane on improvement of learning and memory function.

Astrocytes are key central nervous system components of the injury response, including neonatal asphyxia (Zhao and Rempe, 2010). In the acute phase following HI damage, these glial cells become activated and begin to proliferate. Proliferation of glial cells is crucial for sealing the site of injury, remodeling the hippocampal tissue structure, and temporally and spatially controlling the local immune response; however, this response becomes harmful in the chronic phase (Pekny and Nilsson, 2005; Pekny et al., 2014). Indeed, this excessive astrocyte hypertrophy impairs hippocampal anatomical structures. More specifically, our immunofluorescence results showed that astrocytes around the CA1 and CA3 pyramid layer, as well as in the DG region (especially the border between the granule cell layer and hilum), severely destroyed the normal tissue structure. The processes of glial scaffolds grew into the regular neuron array. Morphological results illustrated that these excessive GFAP-expressing radial glia reoriented their processes into a dense mesh, which formed a wall-like structure that obstructed synapse development and directly impaired spatial-dependent learning and memory (Wanner et al., 2008).

The Morris water maze test, a classic behavior test used to detect hippocampus-related learning and memory (Wu et al., 2018), was combined in this study with immunofluorescence staining results to provide new evidence that sevoflurane could improve learning and memory by reducing excessive astrogliosis and glial scarring. Not only did the immunofluorescence intensity of neurocan and GFAP in hypertrophic astrocytes obviously decrease after SPC, but protein expression levels also decreased. Meanwhile, Nissl staining revealed a denser, more regular hippocampal architecture, hyperchromatic cytoplasm, very little neuronal loss, and marked cellular atrophy after SPC. Golgi staining also provided evidence that SPC could elevate the number of dendritic spines. Another novel finding of this study is that SPC upregulated expression of synaptic markers PSD95 and GAP43 in the hippocampus compared with the HI group. This phenomenon indicates that apart from attenuating glial scars, sevoflurane may facilitate hippocampal synapse formation, which directly improves learning and memory functions (Zhang et al., 2015; Lu et al., 2017).

SPC attenuated glial scarring and excessive astrocyte proliferation in neonatal HIE during development. Dendrite spine numbers can be elevated after SPC, thus providing evidence that sevoflurane can induce synapse formation after HI (Roberts et al., 2010). The application of YC-1, an HIF-1α inhibitor, reversed the therapeutic effect induced by SPC, indicating that the protection of synapse formation is highly related to HIF-1α.

As a crucial transcription factor, HIF-1α has various target genes that perform distinct functions, such as processes involved in cell survival, glucose transport and metabolism, and angiogenesis, after ischemia (Ostrowski and Zhang, 2020). Additionally, HIF-1α expression is tightly regulated by various mechanisms. Previous studies demonstrated that HIF-1α cannot consistently exist in brain tissue at a high, effective level because of the oxygen-dependent ubiquitylation degradation pathway (Hirayama and Koizumi, 2017). Therefore, finding a way to maintain HIF expression levels can extend its protective effects after HI.

Recently, a new treatment modality has been proposed, in which mild hypoxic postconditioning is applied after a period of HI injury to alleviate brain damage (Zhan et al., 2012). Hypoxic postconditioning has been verified to reduce glial activation, including both astrocytes and microglia. Moreover, decreases in inflammatory markers have been observed after hypoxic postconditioning (Teo et al., 2015). The potential mechanism underlying this protection was demonstrated to be closely related to the maintenance of HIF-1α expression (Zhu et al., 2014).

At present, post-conditioning of hypoxia is nearly impossible to apply in clinical practice as a conventional detrimental treatment, and has many potential hazards. Additionally, individual differences in hypoxia tolerance make it difficult to standardize the dose control of hypoxia post-conditioning treatment (Zhan et al., 2012). For neonatal HIE, inaccurate post-conditioning of hypoxia treatment is extremely likely to cause secondary injury. In contrast, sevoflurane is safer, milder, and more controllable in clinical practice, and as demonstrated in our research, can also upregulate HIF-1α expression.

Similar to its neuroprotective role in PD, DJ-1 seems to play an essential role in SPC in our research. The best-defined substrate of VHL, a widely known E3 ubiquitin ligase complex, is HIF-1α (Zhang et al., 2018). DJ-1 has been verified to interact with VHL and can effectively decrease VHL expression, which induces HIF-1α stabilization (Parsanejad et al., 2014). We hypothesized that sevoflurane protects the brain against hypoxic damage by upregulating DJ-1 and inhibiting the ubiquitylation activity of VHL. Our novel findings obtained from real-time PCR and western blot analysis support this hypothesis. First, the difference in HIF-1α between SPC and HI groups did not result from transcriptional alterations. Second, VHL expression decreased while DJ-1 expression increased in the SPC group. Third, stabilization of HIF-1α protected synapse formation and learning and memory function, and reversed astrogliosis and glial scarring. Thus, sevoflurane most likely regulates HIF-1α through inhibition of ubiquitylation by VHL via a DJ-1 interaction.

A previous study showed that HIF-1α plays essential roles in regulation of neural stem progenitor cells and promoting responses to hypoxia (Cunningham et al., 2012). HIF-1α is an intrinsic regulator of neural stem progenitor cell multipotency and developmental outcomes upon differentiation. Further investigation showed that HIF-1α promoted the differentiation of neural stem cells into neurons and inhibited their differentiation into glial cells through regulation of Notch and Wnt signaling pathways in the subventricular zone (Lie et al., 2005; Morris et al., 2007; Kuwabara et al., 2009; Mazumdar et al., 2010). In neonatal rat hippocampus, HIF-1α may also provide neuroprotection by modulating neural progenitor cell differentiation outcomes to attenuate excessive astrogliosis. However, the specific mechanism has yet to be clarified and requires further research.

The current study had several limitations. First, dynamic changes in astrocyte activation were not observed or recorded. Second, the definitive mechanism by which HIF-1α reduces astrogliosis was not investigated. Third, although astrocyte and microglia activation have been observed to occur simultaneously, our study focused on astrocytes instead of microglia activation or the subsequent inflammatory reaction, which would be extremely valuable to investigate. Second, the behavior test performance of female rats was slightly better than that of male rats, and the increase of glial cells of female rats was also slightly less than that of male rats. However, behavior test results of the two sexes showed no statistical differences after sevoflurane post-conditioning. The specific mechanism underlying sex-specific effects on development after HI will be investigated in our future research. In addition, genetic methods such as knockout of the gene encoding DJ-1 would be beneficial in demonstrating whether the neuroprotective effects of SPC treatment result from inhibition of HIF-1α ubiquitylation.

Regardless, our findings indicate that sevoflurane alleviates astrogliosis and glial scar formation in the rat hippocampus, and reduces learning and memory impairment after HI injury by stabilizing HIF-1α expression. This mechanism may be related to sevoflurane-induced upregulation of the neuroprotective protein DJ-1, thus reducing VHL, the ubiquitin ligase of HIF-1α. These findings provide new targets for the treatment of neonatal ischemic hypoxic encephalopathy.

Author contributions: *Study conception and design: PZ and QSG; experimental implementation: QSG, YHZ, and ZYW; data analysis: QSG; providing reagents/materials/analysis tools: HX, CL; paper writing: QSG; statistical expertise, obtaining funding, administrative, technical or material support, and supervision: PZ. All authors approved the final version of the paper.*
Conflicts of interest: *The authors declare that they have no conflict of interest.*
Financial support: *This study was supported by the National Nature Science Foundation of China, Nos. 81671311, 81870838; the Key Research and Development Program of Liaoning Province of China, No. 2018225004; and the Outstanding Scientific Fund of Shengjing Hospital of China, No. 201708 (all to PZ). The funding sources had no role in study conception and design, data analysis or interpretation, paper writing or deciding to submit this paper for publication.*
Institutional review board statement: *The study was approved by the Laboratory Animal Care Committee of China Medical University, China (approval No. 2016PS337K) on November 9, 2016.*
Copyright license agreement: *The Copyright License Agreement has been signed by all authors before publication.*
Data sharing statement: *Datasets analyzed during the current study are available from the corresponding author on reasonable request.*
Plagiarism check: *Checked twice by iThenticate.*
Peer review: *Externally peer reviewed.*

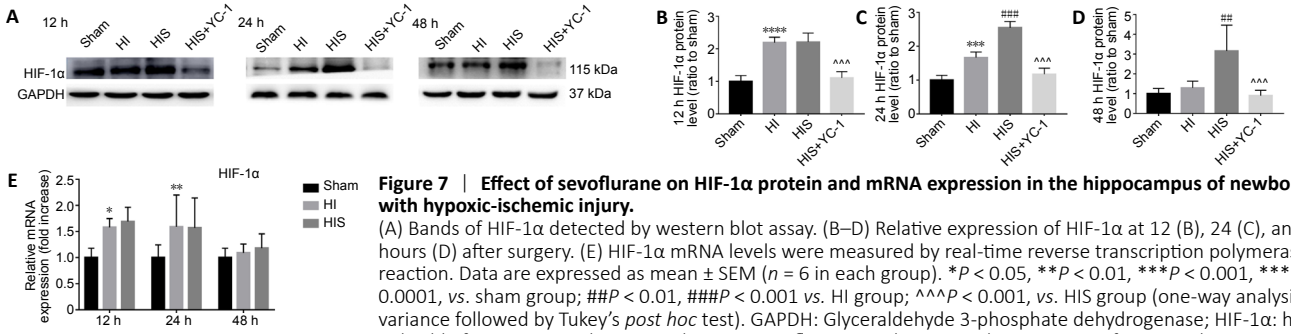

Figure 7 | Effect of sevoflurane on HIF-1α protein and mRNA expression in the hippocampus of newborn rats with hypoxic-ischemic injury.

(A) Bands of HIF-1α detected by western blot assay. (B–D) Relative expression of HIF-1α at 12 (B), 24 (C), and 48 hours (D) after surgery. (E) HIF-1α mRNA levels were measured by real-time reverse transcription polymerase chain reaction. Data are expressed as mean ± SEM (n = 6 in each group). *P < 0.05, **P < 0.01, ***P < 0.001, ****P < 0.0001, *vs.* sham group; ##P < 0.01, ###P < 0.001 *vs.* HI group; ^^^P < 0.001, *vs.* HIS group (one-way analysis of variance followed by Tukey's *post hoc* test). GAPDH: Glyceraldehyde 3-phosphate dehydrogenase; HIF-1α: hypoxia-inducible factor-1α; HIS: hypoxic-ischemic + sevoflurane; HI: hypoxic-ischemic; YC-1: Lificiguat, a hypoxia-inducible factor-1α inhibitor.

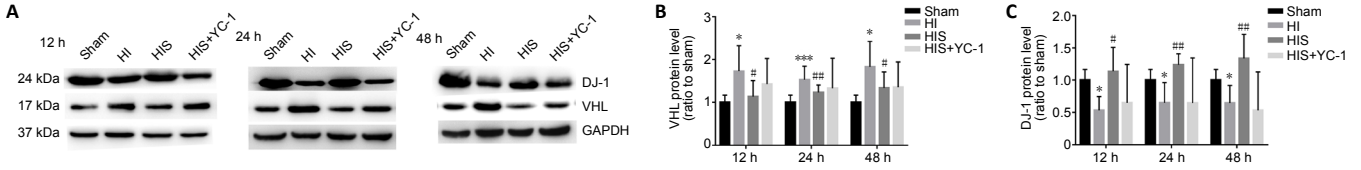

Figure 8 | Effect of sevoflurane on DJ-1 and VHL expression in the hippocampus of newborn rats with hypoxic-ischemic injury after SPC for 12, 24, and 48 hours.

(A) Bands of DJ-1 and VHL detected by western blot assay. (B, C) Relative expression of VHL (B) and DJ-1 (C). Data are expressed as mean ± SEM (n = 6 in each group). *P < 0.05, ***P < 0.001, *vs.* sham group; #P < 0.05, ##P < 0.01, *vs.* HI group (one-way analysis of variance followed by Tukey's *post hoc* test). DJ-1: A neuroprotective protein; GAPDH: glyceraldehyde 3-phosphate dehydrogenase; HIF-1α: hypoxia-inducible factor-1α; HIS: hypoxic-ischemic + sevoflurane; HI: hypoxic-ischemic; VHL: von Hippel-Lindau, E3 ubiquitin ligase complex of hypoxia-inducible factor-1α; YC-1: Lificiguat, a hypoxia-inducible factor-1α inhibitor.

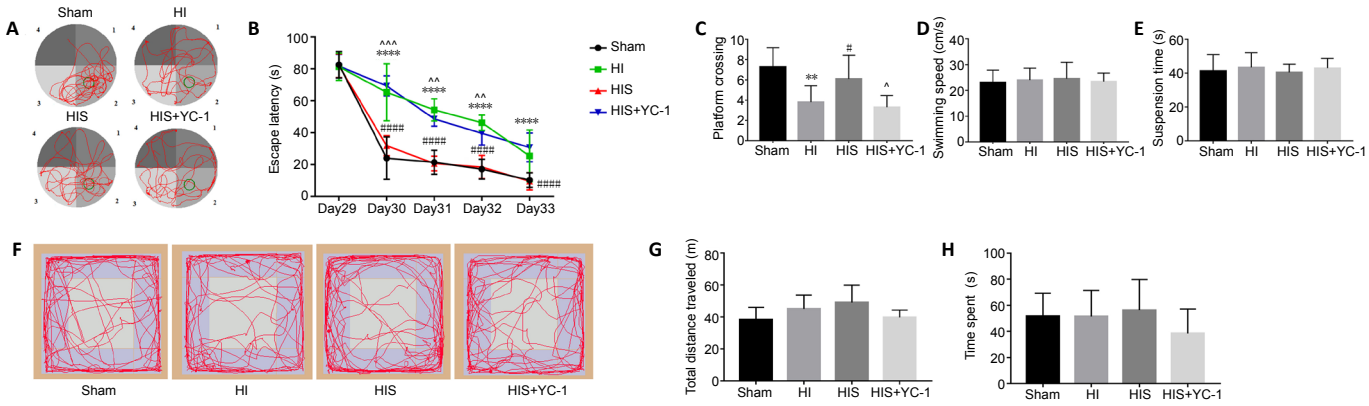

Figure 9 | Effect of sevoflurane on the behavioral function of newborn rats with hypoxic-ischemic injury.

(A) Representative motion track (red lines) of Morris water maze. Green circles indicate the target platform. 1–4: Quadrant 1–4. (B) Escape latency in Morris water maze test. (C) Platform crossing time in Morris water maze test. (D) Swimming speed in Morris water maze test. (E) Suspension latency in suspension test. (F) Representative motion track of the open field test. (G) Total distance traveled in the open field test. (H) Time spent in the central area of the open field test. Data are expressed as mean ± SEM (n = 10). **P < 0.01, ****P < 0.0001, *vs.* sham group; #P < 0.05, ####P < 0.0001, *vs.* HI group; ^P < 0.05, ^^P < 0.01, ^^^P < 0.001, *vs.* HIS group (two-way analysis of variance). HI: Hypoxic-ischemic; YC-1: Lificiguat, a hypoxia-inducible factor-1α inhibitor.

References

Aleyasin H, Rousseaux MW, Phillips M, Kim RH, Bland RJ, Callaghan S, Slack RS, During MJ, Mak TW, Park DS (2007) The Parkinson's disease gene DJ-1 is also a key regulator of stroke-induced damage. Proc Natl Acad Sci U S A 104:18748-18753.

Aleyasin H, Rousseaux MW, Marcogliese PC, Hewitt SJ, Irrcher I, Joselin AP, Parsanejad M, Kim RH, Rizzu P, Callaghan SM, Slack RS, Mak TW, Park DS (2010) DJ-1 protects the nigrostriatal axis from the neurotoxin MPTP by modulation of the AKT pathway. Proc Natl Acad Sci U S A 107:3186-3191.

Archer DP, Walker AM, McCann SK, Moser JJ, Appireddy RM (2017) Anesthetic neuroprotection in experimental stroke in rodents: a systematic review and meta-analysis. Anesthesiology 126:653-665.

Barkhuizen M, van den Hove DL, Vles JS, Steinbusch HW, Kramer BW, Gavilanes AW (2017) 25 years of research on global asphyxia in the immature rat brain. Neurosci Biobehav Rev 75:166-182.

Berra E, Benizri E, Ginouvès A, Volmat V, Roux D, Pouysségur J (2003) HIF prolyl-hydroxylase 2 is the key oxygen sensor setting low steady-state levels of HIF-1alpha in normoxia. EMBO J 22:4082-4090.

Burda JE, Sofroniew MV (2014) Reactive gliosis and the multicellular response to CNS damage and disease. Neuron 81:229-248.

Choudhury GR, Ding S (2016) Reactive astrocytes and therapeutic potential in focal ischemic stroke. Neurobiol Dis 85:234-244.

Cunningham LA, Candelario K, Li L (2012) Roles for HIF-1α in neural stem cell function and the regenerative response to stroke. Behav Brain Res 227:410-417.

Davidson JO, Wassink G, van den Heuij LG, Bennet L, Gunn AJ (2015) Therapeutic hypothermia for neonatal hypoxic-ischemic encephalopathy-where to from here? Front Neurol 6:198.

Davies A, Wassink G, Bennet L, Gunn AJ, Davidson JO (2019) Can we further optimize therapeutic hypothermia for hypoxic-ischemic encephalopathy? Neural Regen Res 14:1678-1683.

Descloux C, Ginet V, Clarke PG, Puyal J, Truttmann AC (2015) Neuronal death after perinatal cerebral hypoxia-ischemia: Focus on autophagy-mediated cell death. Int J Dev Neurosci 45:75-85.

Doi K, Sameshima H, Kodama Y, Furukawa S, Kaneko M, Ikenoue T (2012) Perinatal death and neurological damage as a sequential chain of poor outcome. J Matern Fetal Neonatal Med 25:706-709.

Douglas-Escobar M, Weiss MD (2015) Hypoxic-ischemic encephalopathy: a review for the clinician. JAMA Pediatr 169:397-403.

Du Y, Gong XD, Fang X, Xing F, Xia TJ, Gu XP (2020) Sevoflurane plays a reduced role in cognitive impairment compared with isoflurane: limited effect on fear memory retention. Neural Regen Res 15:96-102.
Edwards AD, Brocklehurst P, Gunn AJ, Halliday H, Juszczak E, Levene M, Strohm B, Thoresen M, Whitelaw A, Azzopardi D (2010) Neurological outcomes at 18 months of age after moderate hypothermia for perinatal hypoxic ischaemic encephalopathy: synthesis and meta-analysis of trial data. BMJ 340:c363.
Grandvuillemin I, Garrigue P, Ramdani A, Boubred F, Simeoni U, Dignat-George F, Sabatier F, Guillet B (2017) Long-term recovery after endothelial colony-forming cells or human umbilical cord blood cells administration in a rat model of neonatal hypoxic-ischemic encephalopathy. Stem Cells Transl Med 6:1987-1996.
Hirayama Y, Koizumi S (2017) Hypoxia-independent mechanisms of HIF-1α expression in astrocytes after ischemic preconditioning. Glia 65:523-530.
Hopkins RO, Haaland KY (2004) Neuropsychological and neuropathological effects of anoxic or ischemic induced brain injury. J Int Neuropsychol Soc 10:957-961.
Jevtovic-Todorovic V, Hartman RE, Izumi Y, Benshoff ND, Dikranian K, Zorumski CF, Olney JW, Wozniak DF (2003) Early exposure to common anesthetic agents causes widespread neurodegeneration in the developing rat brain and persistent learning deficits. J Neurosci 23:876-882.
Jung S, Choe S, Woo H, Jeong H, An HK, Moon H, Ryu HY, Yeo BK, Lee YW, Choi H, Mun JY, Sun W, Choe HK, Kim EK, Yu SW (2020) Autophagic death of neural stem cells mediates chronic stress-induced decline of adult hippocampal neurogenesis and cognitive deficits. Autophagy 16:512-530.
Kim HC, Kim E, Bae JI, Lee KH, Jeon YT, Hwang JW, Lim YJ, Min SW, Park HP (2017) Sevoflurane postconditioning reduces apoptosis by activating the JAK-STAT pathway after transient global cerebral ischemia in rats. J Neurosurg Anesthesiol 29:37-45.
Kuwabara T, Hsieh J, Muotri A, Yeo G, Warashina M, Lie DC, Moore L, Nakashima K, Asashima M, Gage FH (2009) Wnt-mediated activation of NeuroD1 and retro-elements during adult neurogenesis. Nat Neurosci 12:1097-1105.
Lai Z, Zhang L, Su J, Cai D, Xu Q (2016) Sevoflurane postconditioning improves long-term learning and memory of neonatal hypoxia-ischemia brain damage rats via the PI3K/Akt-mPTP pathway. Brain Res 1630:25-37.
Lie DC, Colamarino SA, Song HJ, Désiré L, Mira H, Consiglio A, Lein ES, Jessberger S, Lansford H, Dearie AR, Gage FH (2005) Wnt signalling regulates adult hippocampal neurogenesis. Nature 437:1370-1375.
Liu YP, Gong XF (2020) Effects of dexmedetomidine on perioperative brain protection in patients undergoing craniocerebral surgery under inhalation anesthesia with sevoflurane: a randomized controlled study. Zhongguo Zuzhi Gongcheng Yanjiu 24:5688-5694.
Lu H, Liufu N, Dong Y, Xu G, Zhang Y, Shu L, Soriano SG, Zheng H, Yu B, Xie Z (2017) Sevoflurane acts on ubiquitination-proteasome pathway to reduce postsynaptic density 95 protein levels in young mice. Anesthesiology 127:961-975.
Mazumdar J, O'Brien WT, Johnson RS, LaManna JC, Chavez JC, Klein PS, Simon MC (2010) O2 regulates stem cells through Wnt/β-catenin signalling. Nat Cell Biol 12:1007-1013.
Morris AM, Churchwell JC, Kesner RP, Gilbert PE (2012) Selective lesions of the dentate gyrus produce disruptions in place learning for adjacent spatial locations. Neurobiol Learn Mem 97:326-331.
Morris DC, Zhang ZG, Wang Y, Zhang RL, Gregg S, Liu XS, Chopp M (2007) Wnt expression in the adult rat subventricular zone after stroke. Neurosci Lett 418:170-174.
Na JI, Na JY, Choi WY, Lee MC, Park MS, Choi KH, Lee JK, Kim KT, Park JT, Kim HS (2015) The HIF-1 inhibitor YC-1 decreases reactive astrocyte formation in a rodent ischemia model. Am J Transl Res 7:751-760.
Ostrowski RP, Zhang JH (2020) The insights into molecular pathways of hypoxia-inducible factor in the brain. J Neurosci Res 98:57-76.
Parsanejad M, Zhang Y, Qu D, Irrcher I, Rousseaux MW, Aleyasin H, Kamkar F, Callaghan S, Slack RS, Mak TW, Lee S, Figeys D, Park DS (2014) Regulation of the VHL/HIF-1 pathway by DJ-1. J Neurosci 34:8043-8050.
Paxinos G, Franklin KB (2013) The mouse brain in stereotaxic coordinates. San Diego: Elsevier.
Pekny M, Nilsson M (2005) Astrocyte activation and reactive gliosis. Glia 50:427-434.
Pekny M, Wilhelmsson U, Pekna M (2014) The dual role of astrocyte activation and reactive gliosis. Neurosci Lett 565:30-38.
Roberts TF, Tschida KA, Klein ME, Mooney R (2010) Rapid spine stabilization and synaptic enhancement at the onset of behavioural learning. Nature 463:948-952.
Rolls A, Shechter R, Schwartz M (2009) The bright side of the glial scar in CNS repair. Nat Rev Neurosci 10:235-241.
Shen F, Li YJ, Shou XJ, Cui CL (2012) Role of the NO/sGC/PKG signaling pathway of hippocampal CA1 in morphine-induced reward memory. Neurobiol Learn Mem 98:130-138.
Shi Y, Yi C, Li X, Wang J, Zhou F, Chen X (2017) Overexpression of Mitofusin2 decreased the reactive astrocytes proliferation in vitro induced by oxygen-glucose deprivation/reoxygenation. Neurosci Lett 639:68-73.
Stankowski JN, Gupta R (2011) Therapeutic targets for neuroprotection in acute ischemic stroke: lost in translation? Antioxid Redox Signal 14:1841-1851.
Teo JD, Morris MJ, Jones NM (2015) Hypoxic postconditioning reduces microglial activation, astrocyte and caspase activity, and inflammatory markers after hypoxia-ischemia in the neonatal rat brain. Pediatr Res 77:757-764.
Wang R, Zhang X, Zhang J, Fan Y, Shen Y, Hu W, Chen Z (2012) Oxygen-glucose deprivation induced glial scar-like change in astrocytes. PLoS One 7:e37574.
Wang S, Xue H, Xu Y, Niu J, Zhao P (2019a) Sevoflurane postconditioning inhibits autophagy through activation of the extracellular signal-regulated kinase cascade, alleviating hypoxic-ischemic brain injury in neonatal rats. Neurochem Res 44:347-356.
Wang T, Zeng LN, Zhu Z, Wang YH, Ding L, Luo WB, Zhang XM, He ZW, Wu HF (2019b) Effect of lentiviral vector-mediated overexpression of hypoxia-inducible factor 1 alpha delivered by pluronic F-127 hydrogel on brachial plexus avulsion in rats. Neural Regen Res 14:1069-1078.
Wanner IB, Deik A, Torres M, Rosendahl A, Neary JT, Lemmon VP, Bixby JL (2008) A new in vitro model of the glial scar inhibits axon growth. Glia 56:1691-1709.
Wu Z, Li X, Zhang Y, Tong D, Wang L, Zhao P (2018) Effects of sevoflurane exposure during mid-pregnancy on learning and memory in offspring rats: beneficial effects of maternal exercise. Front Cell Neurosci 12:122.
Xue H, Xu Y, Wang S, Wu ZY, Li XY, Zhang YH, Niu JY, Gao QS, Zhao P (2019) Sevoflurane post-conditioning alleviates neonatal rat hypoxic-ischemic cerebral injury via Ezh2-regulated autophagy. Drug Des Devel Ther 13:1691-1706.
Yang L, Wu J, Xie P, Yu J, Li X, Wang J, Zheng H (2019) Sevoflurane postconditioning alleviates hypoxia-reoxygenation injury of cardiomyocytes by promoting mitochondrial autophagy through the HIF-1/BNIP3 signaling pathway. PeerJ 7:e7165.
Yiu G, He Z (2006) Glial inhibition of CNS axon regeneration. Nat Rev Neurosci 7:617-627.
Yuan J (2009) Neuroprotective strategies targeting apoptotic and necrotic cell death for stroke. Apoptosis 14:469-477.
Zhai F, Shi F, Wang J, Dai CF, Fan C (2019) Preliminary study on the mechanism underlying the interaction of balance dysfunction and anxiety disorder. Neuroreport 30:53-59.
Zhan L, Li D, Liang D, Wu B, Zhu P, Wang Y, Sun W, Xu E (2012) Activation of Akt/FoxO and inactivation of MEK/ERK pathways contribute to induction of neuroprotection against transient global cerebral ischemia by delayed hypoxic postconditioning in adult rats. Neuropharmacology 63:873-882.
Zhang J, Dong Y, Zhou C, Zhang Y, Xie Z (2015) Anesthetic sevoflurane reduces levels of hippocalcin and postsynaptic density protein 95. Mol Neurobiol 51:853-863.
Zhang W, Li Q, Li D, Li J, Aki D, Liu YC (2018) The E3 ligase VHL controls alveolar macrophage function via metabolic-epigenetic regulation. J Exp Med 215:3180-3193.
Zhao P, Peng L, Li L, Xu X, Zuo Z (2007) Isoflurane preconditioning improves long-term neurologic outcome after hypoxic-ischemic brain injury in neonatal rats. Anesthesiology 107:963-970.
Zhao Y, Rempe DA (2010) Targeting astrocytes for stroke therapy. Neurotherapeutics 7:439-451.
Zhu T, Zhan L, Liang D, Hu J, Lu Z, Zhu X, Sun W, Liu L, Xu E (2014) Hypoxia-inducible factor 1α mediates neuroprotection of hypoxic postconditioning against global cerebral ischemia. J Neuropathol Exp Neurol 73:975-986.

C-Editor: Zhao M; S-Editors: Yu J, Li CH; L-Editors: Yu J, Song LP; T-Editor: Jia Y